Effects of nitrate/ammonium nitrogen ratio or deficient nitrogen nutrition on photosynthesis and oxalate parameters of hydroponically grown pigweed (Amaranthus hybridus)

Aristofanis Matiatos
Dimosthenis Nikolopoulos
Panagiota Bresta
Michail Lykouras
Malvina G. Orkoula
Christos G. Kontoyannis
George Grammatikopoulos
Evangelos-Alexandros Kyrkoulis
Oltian Moutsa
George Karabourniotis
Georgios Liakopoulos

gliak@aua.gr

Agricultural University of Athens

Research Article

Keywords: nitrogen nutrition, nitrate, ammonium, pigweed (Amaranthus hybridus), calcium oxalate, photosynthesis

Posted Date: February 9th, 2026

DOI: https://doi.org/10.21203/rs.3.rs-8740762/v1

Abstract

Background and Aims

: The nitrogen (N) form absorbed and assimilated by plants affects many aspects of their physiology including soluble oxalate and calcium oxalate (CaOx) crystals. Based on the above relationship, attempts have been made to reduce the oxalate content of plants used for human consumption or animal feed by controlling nutrition.

Methods

The effects of N form in hydroponically grown pigweed (*Amaranthus hybridus*) plants using different NO_3^-/NH_4^+ ratios (1:0, 1:1 or 1:3; always summing to 7.5 m*M* in nutrient solution) or deficient levels of N (0.5 m*M* NO_3^-) were studied. The changes in oxalate physiology including CaOx crystals' number, size and chemical composition, leaf and root soluble and insoluble oxalate content, and root oxalate exudation were examined. Also, the effects of N nutrition on photosynthesis were studied considering its association with both N and CaOx crystals, the latter particularly in photosynthesis under stress, also known as alarm photosynthesis.

Results

Increase of NH_4^+ supply resulted in a dramatic decrease in insoluble and, much more in, soluble oxalate. Photosynthetic rate showed a reducing trend while, in contrast, JIP-test chlorophyll fluorescence parameters were improved. Deficient supply of NO_3^--N resulted in considerable negative effects in photosynthesis while oxalate parameters were not affected to a notable extend.

Conclusion

Pigweed is not impaired by N nutrition indicating its facultative calcicole physiotype and wide ecological adaptation, compatible with its cosmopolitan distribution. A direct interaction between oxalate physiology and N nutrition is evident, while those with photosynthesis are much more puzzling, yielding future research questions.

Introduction

Plants produce and store oxalate, a multifunctional carbon metabolite involved in several essential regulatory, protective and defensive functions of both underground and above ground parts (Karabourniotis et al. 2020, Li et al. 2022). Usually, leaves show the highest concentrations of oxalate of all plant organs (Nakata 2012), which is either synthesized locally or transferred via the xylem

(Karabourniotis et al. 2020; Li et al. 2022). Despite its abundance, soluble oxalate concentrations must be precisely controlled to avoid growth impediment and other physiological perturbations (Kumar et al. 2019; Li et al. 2022), while excess amounts are deposited as oxalate salts. Oxalate itself contributes to the control of calcium (Ca) ions, another cellular constituent which also arrives in plant tissues via the xylem and its cellular concentration must be tightly regulated (Paiva 2019). Together, these two components form Ca oxalate (CaOx) crystals, usually deposited inside the vacuoles of many cell types including specialised idioblastic cells called crystal cells (Franceschi 1987), although extracellular deposition is also common (Kumar et al. 2019). Crystal cells often contain very large CaOx crystals reaching a diameter of 50 μm or more (Karabourniotis et al. 2020).

Possible roles of soluble oxalate include Ca regulation, ionic, pH and osmotic homeostasis (Palmieri et al. 2019; Raven and Smith 1976). Both nitrate-nitrogen (N) accumulation and excess cation uptake tend to increase, while anion uptake or synthesis of organic anions tend to decrease cellular pH, the latter being part of the cellular pH-stat (Raven and Smith 1976). Oxalate accumulation has the advantage that being deposited as insoluble CaOx is osmotically inactive (Libert and Franceschi 1987). Oxalate has also been associated with resistance against pathogens (Kumar et al. 2019; Palmieri et al. 2019) and abiotic stress factors such as metal toxicity and cold (Li et al. 2022). CaOx crystals constitute a dynamic system exhibiting diurnal (Karabourniotis et al. 2020; Tooulakou et al. 2016a, b) and stress-specific variations (Karabourniotis et al. 2020; Paiva 2019; Tooulakou et al. 2016a, b, 2019). The underlying rationale for this system appears to involve carbon recycling through suggested alarm photosynthesis-type processes (Karabourniotis et al. 2020; Tooulakou et al. 2016a, b), while the possibility of Ca recycling seems less plausible, as a more reasonable and effective form of Ca recycling would likely need to be on a whole-plant level, which is not supported by the restricted phloem mobility of Ca^{2+} ions (Paiva 2019).

Despite its ubiquitous presence, soluble oxalate and CaOx crystals are unwanted components in foodstuff, as they represent antinutrient factors (Libert and Franceschi 1987; Massey 2003). Oxalate in edible parts of vegetables, food and forage crops lowers the nutritional quality and raises health concerns because it decreases Ca bioavailability by forming CaOx crystals, which can lead to kidney stones formation (Franceschi and Nakata 2005; Libert and Franceschi 1987; Massey 2003). The measures proposed for reducing oxalate in crop plants include genetic means, such as plant genotype selection, metabolic engineering and other biotechnology means, such as inhibiting the activity of oxalate precursor enzymes or enhancing the activity of oxalate degradation enzymes (Kumar et al. 2019; Li et al. 2022). Other proposed measures include agricultural practices, such as adjusting planting time, increasing growth rate and controlling of N, potassium and Ca nutrition (Li et al. 2022; Libert and Franceschi 1987). The regulation of oxalate levels by N nutrition in selected crops is promising, especially considering the increasing trend of hydroponic plant production systems. This method can increase the nutritional value of oxalate accumulating vegetables (such as spinach, sugar beet, amaranths etc.) by enhancing the dietary bioavailability of Ca and other minerals while reducing health risks (Franceschi and Nakata 2005; Libert and Franceschi 1987; Massey 2003).

It has been long documented (see Libert and Franceschi 1987 and references therein) that nitrate uptake and assimilation, in the root, shoot or both (Raven and Smith 1976; Xu et al. 2006), leads to the accumulation of carboxylate anions. Oxalate is the preferred form of such a homeostatic mechanism in many plant species (Raven and Smith 1976). It is commonly reported that oxalate accumulation is much less when ammonium is the primary or sole N supply (Al Daini et al. 2013; Goyal and Kaur 2019; Ji and Peng 2005; Libert and Franceschi 1987; Liu et al. 2015a; Morita et al. 2004; Sugiyama and Okutani 1996; Tian et al. 2008; Zhang et al. 2005), indicating that nitrate reduction induces oxalate build-up.

The interaction between soil nutrients, accumulation of oxalate and formation of CaOx crystals is a complex process depending strongly on the Ca physiotype of each species. Ecologists have classified plant species into two different Ca physiotypes, the calcifuges and the calcicoles (White and Broadley 2003). Calcicole species are adapted to thrive on Ca-rich soils (calcareous soils). These soils are characterized by high Ca concentrations which may stimulate their growth but are saturating or inhibitory for calcifuge species (Lambers et al. 2019; White and Broadley 2003). High Ca concentrations are usually accompanied by high pH values and high (bi)carbonate concentrations. Calcifuge species on the other hand have a distinct preference for soils with low pH and low Ca levels. These plants are usually restricted to acid soils because they lack the capacity to acquire some nutrients from alkaline soils and to avoid excessive uptake of Ca. On the other hand, calcicoles are restricted to Ca-rich and often alkaline soils, because they are adversely affected by excessive aluminum, manganese and iron (Fe) levels in acid soils (Lambers et al. 2019). Calcicoles thriving in calcareous soils must cope with the limited availability of certain nutrients (Bothe 2015). For this reason, they are capable to mobilize poorly available nutrients (e.g., Fe, phosphorus, and zinc) by secreting organic acids (including oxalate) from their roots (Jones 1998; Lee 1998; Ström 1997; Tyler and Ström 1995). Moreover, because of their higher porosity, calcareous soils often have a much lower water-holding capacity than acidic soils (Michalet et al. 2002). Consequently, calcicoles must cope with more intense drought conditions, compared to those growing on acidic soil, and often show a higher drought tolerance than typical calcifuge species (Bothe 2015; Michalet et al. 2002; Nemer et al. 2021). The solubilisation of nutrients by organic acids' exudation inevitably enhances the availability of Ca, therefore the xylem sap of calcicoles may contain high concentrations of the element (such in members of Crassulaceae, Brassicaceae and Fabaceae). Many calcicoles can control Ca cellular concentration by precipitating excess amounts in the form of CaOx crystals (Kinzel and Lechner 1992; Lee 1998). Although detailed studies on this subject are absent, it seems that the formation of these crystals is related to the Ca requirements of each plant species. For example, the Ca requirement for optimal growth is much higher in dicotyledons (e.g., soybean, bean, cotton, sugar beet and sunflower) than in monocotyledons (including many cereals such as rice, maize, wheat and sorghum) (Marschner 1974; White and Broadley 2003). Consequently, CaOx crystals in cereals and related taxonomic groups are absent (Prychid and Rudall 1999), whereas they exist in plethora in dicotyledons.

This study aims to investigate the effect of different types of N nutrition (different NO_3^-/NH_4^+ ratios or deficient nitrate supply) on photosynthesis and oxalate physiology of pigweed (*Amaranthus hybridus*), an

oxalate accumulating species (Kinzel and Lechner 1992). Pigweed is a cosmopolitan species, considered as a weed and is also an edible herb, extensively consumed in many parts of the world (Peña and Minguez 2024). It has been studied extensively to gain an insight to the ecophysiological role of CaOx crystals in carbon metabolism and photosynthesis (Tooulakou et al. 2016a, b, 2019). The examination of the effects of N form on CaOx crystals and photosynthesis thus, increases the potential interest of this study.

Materials and Methods

Plant material and growth conditions

Pigweed (*Amarathus hybridus* L.) seeds were sown on perlite in petri dishes under dim light and transplanted after 14 d in pots filled with perlite (provided with a commercial fertilizer; Gemma 20-20-20 plus micronutrients; 0.14 g l^{-1}) inside a growth chamber. Light was provided by Powerstar HQI-BT-400W/D (OSRAM), photosynthetically active radiation (PAR) photon flux density (PFD) was 120 µmol (quanta) m^{-2} s^{-1}, photoperiod was 16/8h, day/night temperature was 22/18°C, and air relative humidity was ca. 75%. Forty days after sowing, 24 healthy and uniform plants were transferred to four types of aerated nutrient solutions in 1 L containers (six replicates per treatment) and grown hydroponically for a period of 50 days (main experimental period) under the same environmental conditions.

Treatments were: 7.5 m*M* N, NO_3^-/NH_4^+ ratio of 1:0, symbolized as 'NO_3'; 7.5 m*M* N, NO_3^-/NH_4^+ ratio of 1:1, symbolized as 'NO_3/NH_4'; 7.5 m*M* N, NO_3^-/NH_4^+ ratio of 1:3, symbolized as 'NH_4' and 0.5 m*M* N, NO_3^-/NH_4^+ ratio of 1:0, symbolized as '-NO_3'. Nutrient solutions were based on half strength Hoagland No. 2 modified to each NO_3^-/NH_4^+ ratio as follows: 'NO_3': 3 m*M* KNO_3, 1 m*M* KH_2PO_4, 0.25 m*M* K_2SO_4, 2.25 m*M* $Ca(NO_3)_2$, 1 m*M* $MgSO_4$. 'NO_3/NH_4': 2 m*M* KNO_3, 1 m*M* KH_2PO_4, 0.5 m*M* K_2SO_4, 0.875 m*M* $Ca(NO_3)_2$, 1.13 m*M* $CaSO_4$, 1 m*M* $MgSO_4$, 1.5 m*M* $(NH_4)_2SO_4$, 0.75 m*M* $NH_4H_2PO_4$. 'NH_4': 1 m*M* KNO_3, 1 m*M* KH_2PO_4, 1 m*M* K_2SO_4, 0.435 m*M* $Ca(NO_3)_2$, 1.575 m*M* $CaSO_4$, 1 m*M* $MgSO_4$, 2.57 m*M* $(NH_4)_2SO_4$, 0.5 m*M* $NH_4H_2PO_4$. '-NO_3': 1 m*M* KH_2PO_4, 1.5 m*M* K_2SO_4, 0.25 m*M* $Ca(NO_3)_2$, 1.75 m*M* $CaSO_4$, 1 m*M* $MgSO_4$. Micronutrient concentrations were the same for all treatments: 50 µ*M* Fe-EDTA, 23 µ*M* H_3BO_3, 4.6 µ*M* $ZnSO_4$, 0.16 µ*M* $CuSO_4$, 0.06 µ*M* Na_2MoO_4. pH values were adjusted to 6.5 using a dilute KOH solution. All chemicals were of analytical grade (Merck KGaA, Darmstadt, Germany). Solutions were replaced every 3–4 days.

All tissue samples for chemical analyses were collected at the end of the main experimental period and stored at -80°C until processing. Xylem sap was collected from the exudate at the cut end between root and stem using a plastic pipettes, after discarding the first few tenths of microlitres. All liquid samples of xylem sap and nutrient solutions were kept at 4°C until processing. Fresh leaf samples for CaOx crystal isolation or for measurements or crystal density and size were collected and processed immediately as described below.

Photosynthetic parameters

All photosynthesis related parameters were measured between 09:00 and 13:00 hours during two days at the end of the main experimental period.

Chlorophyll *a* fluorescent transients (OJIP curves) were recorded by continuous excitation chlorophyll fluorescence using a portable chlorophyll fluorimeter (Handy PEA, Hansatech Instruments Ltd., UK). All measurements were conducted on fully expanded leaves after dark adaptation for 30 min. A bank of three red led emitting diodes (LEDs) providing a PFD or 3,000 μmol m^{-2} s^{-1} (peak at 650 nm) was used for chlorophyll excitation. Fluorescence was recorded from 10 μs to 2 s using variable sampling rate according to the default setup of the instrument. Fluorescence data were then transformed in a logarithmic time scale and the derived polyphasic curve was analysed according to the JIP-test protocol (Ceppi et al. 2011; Stirbet and Govindjee 2011; Stirbet et al. 2018; Strasser et al. 2004). The following fluorescence yields (FY) were recorded: maximum (F_m, all reaction centres (RCs) are closed), minimum (F_0, all RCs are open), FY at 2 and 30 ms, at the J and I steps (F_J and F_I respectively), and at 300 μs ($F_{300\mu s}$). Relative variable fluorescence at steps J [$V_J = (F_J - F_0)/(F_m - F_0)$], I [$V_I = (F_I - F_0)/(F_m - F_0)$], and at 300 μs [$V_K = (F_K - F_0)/(F_m - F_0)$] were derived. M_0 is the slope of the normalized curve at the origin of the fluorescence rise [$M0 = 4 (F_{300\mu s} - F_0) \times (F_m - F_0)$. Definitions of parameters are as follows: $\varphi P_0 = TR_0/ABS = F_m - F_0/F_m$, maximum quantum yield of primary PSII photochemistry; $\psi E_0 = ET_0/TR_0 = 1 - V_J$, efficiency by which a PSII trapped electron is transferred from Q_A to Q_B; $\varphi E_0 = ET_0/ABS = 1 - F_J/F_m = \varphi P_0 \times \psi E_0$, quantum yield of the electron transport flux from Q_A to Q_B; $\varphi R_0 = RE_0/ABS = 1 - F_I/F_m = \varphi P_0 \times \psi E_0 \times \delta R_0$, quantum yield for reduction of end electron acceptors at the PSI acceptor side; $\varphi D_0 = 1 - TR_0/ABS = 1 - \varphi P_0 = F_0/F_m$, quantum yield of energy dissipation; $ABS/RC = (M_0/V_J) \times (1/\varphi P_0)$, absorbed photon flux per active reaction centre; $TR_0/RC = M_0/V_J$, trapped excitation flux (leading to Q_A reduction) per active reaction centre; $ET_0/RC = (M_0/V_J) \times (1 - V_J)$, electron transport flux (further than Q_A) per active reaction centre; $DI_0/RC = (ABS/RC - TR_0/RC)$, dissipated energy flux per active reaction centre; $1 - V_I = (F_m - F_I)/(F_m - F_0)$, a measure of relative amplitude of the IP phase in OJIP transient, related to the size of the pools of final PSI electron acceptors; $V_K/V_J = (F_{300\mu s} - F_0)/(F_J - F_0)$, a measure of the relative amplitude of K-band, related to oxygen evolving complex inactivation; $PI_{ABS} = (RC/ABS) \times \varphi P_0/(1 - \varphi P_0) \times \psi E_0/(1 - \psi E_0)$, potential for energy conservation from absorbed exciton to the reduction of Q_B, also termed performance index on absorption basis; $PI_{total} = PI_{ABS} \times \delta R_0/(1 - \delta R_0)$, potential for energy conservation from absorbed exciton to the reduction of PSI end acceptors, also termed total performance index.

Gas exchange parameters were measured by recording light-response curves under growth chamber conditions (concentration of CO_2 540 μmol mol^{-1} air; air temperature in leaf chamber 22.5°C; PFD 0-550 μmol (quanta) m^{-2} s^{-1} using the red-blue LED light source of the leaf measuring head; three min acclimation time under each PFD level; n = 12: 2 leaves × 6 plants) using a portable IRGA photosynthesis instrument (LC Pro+, ADC Bioscientific, UK).

For the photometric determination of chlorophylls, leaf disks of total surface of 1.5 cm^2 were isolated using a cork borer and homogenized using a mortar and pestle. Pigments were extracted using a total of 7–8 mL of ice-cold aqueous acetone 80%. To facilitate homogenization, a small quantity of extraction sand was added together with 50 mg of $CaCO_3$ to protect chlorophylls from plant tissue acids. The extract was kept in ice until centrifugation (2600 × g, 10 min) and supernatants' volume was measured. Optical density of the extracts was measured at 663 and 647 nm in a UV 160A dual beam spectrophotometer (Shimadzu Co., Tokyo, Japan) and chlorophylls were quantified according to Lichtenthaler (1987).

Measurements of CaOx crystal density and size

Crystal density and size were measured in leaf disks bleached in sodium hypochlorite solution (2%) for 24 h. Images of crystals in chlorine-bleached leaves were obtained using a Axiolab microscope (Carl Zeiss, Germany) equipped with a digital camera (DSC-S75; Sony Copr., Japan), and dimensions were measured using ImageJ digital image analysis software (National Institutes of Health, USA; imagej.net).

Isolation and chemical analysis of CaOx crystals

CaOx crystals were isolated to a single combined sample for each treatment by leaf tissue rupture in a homogenizer with isopropanol. After crystal precipitation, the pellet was cleared by sequential washings with pure isopropanol until microscopic observation revealed the absence of cell debris (Tooulakou et al. 2019).

Analyses were performed in a micro-Raman LabRAM HR Evolution spectrometer combined with the ParticleFinder™ software (Horiba Scientific, France). A 532 nm excitation laser was employed for the acquisition of the Raman spectra and its power was set at 100% of its nominal power (100 mW). The exposure time was adjusted at 1 s, while each spectrum was the average result of 5 accumulations. The spectrograph centre was regulated at 1000 cm^{-1}, the value of binning was set at 2, the confocal hole at 100 μm and a 600 gr mm^{-1} grating was selected. The spectrometer was equipped with an air-cooled CCD detector and Olympus objective lenses. The 10× objective lens (NA: 0.25) was used for the measurements.

For each measurement 10 μL of the sample were placed on the surface of a 2.6 cm × 7.6 cm gold-coated glass slide (EMF Corporation, Ithaca, NY, USA) with a thickness of 1.0 mm, offering high reflection. The slides constituted of a titanium layer (50 Å) used as a binder between the glass of the slide and the gold coating and the external layer of bare gold (1000 Å). The sample was allowed to dry at ambient conditions for approximately 5 min. Subsequently, an area of 5×5 mm^2 was viewed using the mosaic module and the existed particles were automatically identified by ParticleFinder™ software (Horiba Scientific, France). All recognised particles were irradiated with the 532 nm laser and their spectra were chemically characterized using KnowItAll (Wiley Science Solutions, USA). The size of the

particles was also automatically measured by ParticleFinder™ software and separate particle size distributions were generated for each chemical identity.

Measurement of oxalate concentration

Soluble and insoluble oxalate concentration was measured using high performance liquid chromatography (HPLC) according to (Savage and Dubois 2006) with modifications. Briefly, freshly thaw samples of leaves or roots (0.4-2.0 g f.w.) were ground in a mortar and extracted with 10 mL H_2O (HPLC grade, Fischer Chemical). Extracts were centrifuged (2600 × g, 10 min) and supernatants were used for soluble oxalate determination. Pellets were suspended and extracted with 10 mL 0.2 N HCl (ChemLab Analytical, Belgium) in a shaking bath at 80°C for 20 min. Extracts were centrifuged and supernatants were used for insoluble oxalate determination. Tissue extracts, xylem sap and nutrient solution samples were filtered through a 0.22 µm cellulose acetate syringe filter (Macherey-Nagel, Germany) prior to HPLC injection. The HPLC system consisted of a DGU-20A5 degasser, a LC-20AD pump, a CTO-20A thermostated column compartment and a SPD-M20A photo-diode array detector (Prominence HPLC System, Shimadzu Co., Japan). An aliquot of 20 µL sample was injected using a Rheodyne 7725i injection valve (Rheodyne Inc., CA, USA) and separated in a 300 mm × 7.8 mm Rezex ion exchange column (Phenomenex Inc., CA, USA) at 40°C, using an isocratic elution at 0.5 mL min^{-1} with 25 m*M* sulphuric acid (PanReac Química SLU, Spain) as the mobile phase. Peaks were detected at 210 nm. The oxalate peak was eluted at 10.4 min and was identified by comparison of the retention time of oxalic acid dihydrate standard (Merck). Reference curves were prepared using standard solutions of oxalate of concentrations between 0.01 and 2 mg mL^{-1} in water or 0.2 N HCl. The water and HCl curves were identical and merged to a single one ($n = 20$; $r^2 = 0.99$).

Statistics

Statistical analyses were performed using PAST (ver. 4.04, Hammer *et al*., 2001). Data were tested for normality (Shapiro-Wilk, at $p < 0.05$) and for homogeneity of variance (Levene's, at $p < 0.05$). When both assumptions were met, we conducted one-way analysis of variance, followed by Tukey's honestly significant difference post hoc test for pairwise comparisons. When either assumption was violated and data transformation did not resolve the violation, a non-parametric Kruskal-Wallis test was applied, followed by Dunn's *post hoc* test.

Results

Photosynthetic parameters

Treatments of different N nutrition resulted in changes in critical photosynthetic parameters. Total chlorophyll concentration increased in the NH_4 treatment compared to the NO_3 treatment, although non-significantly, while decreased significantly in the -NO_3 treatment. A_n showed a decreasing trend by the

increase in NH_4^+ supply (particularly decreased in the NH_4 treatment) but differences were not statistically significant, while g_s and E were not affected. The last two parameters were also not affected by the -NO_3 treatment despite that A_n was less than half of the value of the NO_3 plants (Table 1).

A range of JIP-test derived photochemical indices were evaluated for a better insight of photosynthesis (Fig. 1 and Supplementary Fig. S1). All quantum yields related to primary photochemistry, electron flow and reduction of end electron acceptors at the PSI acceptor side (φP_0, φE_0 and φR_0) increased more or less by the increase in NH_4^+ supply compared to the NO_3 treatment. The efficiency at which an electron moves further than PSII to intersystem electron carriers (ψE_0) was also increased by the increase in NH_4^+ supply. Nearly all the above energy efficiency parameters decreased sharply in the deficient treatment (-NO_3) to about half of the NO_3 treatment's corresponding values (Fig. 1 and Supplementary Fig. S1). The quantum yield of energy dissipation (φD_0) gradually decreased by the increase in NH_4^+ supply while no difference was noted in the deficient treatment (-NO_3) compared to the NO_3 treatment.

The relative amplitude of K-band parameter V_K/V_J was slightly reduced due to the addition of NH_4^+ (NO_3/NH_4 and NH_4 treatments) while increased significantly in the -NO_3 treatment. On the other hand, a significant increase was observed in the relative amplitude of the IP phase in OJIP transient (1-V_I) due to the addition of NH_4^+, while a notable decrease was observed in the -NO_3 treatment (Fig. 1 and Supplementary Fig. S1).

Specific energy fluxes per PSII active reaction centre (ABS/RC, TR_0/RC, ET_0/RC and DI_0/RC) were also affected. Absorption exergy flux (ABS/RC) and trapped energy flux (TR_0/RC) per active reaction centre were reduced by the increase in NH_4^+ supply compared to the NO_3 treatment while electron transport flux per active reaction centre (ET_0/RC) was increased, more prominently in the NH_4 treatment, compared to the NO_3 treatment. Dissipated energy flux per active reaction centre (DI_0/RC) was decreased by the increase in NH_4^+ supply (Fig. 1 and Supplementary Fig. S1).

Energy flux parameters were negatively affected in the nitrate deficient treatment (-NO_3). Specifically, ABS/RC, TR_0/RC were increased while ET_0/RC was notably decreased compared to the sufficient nitrate supply plants (NO_3 treatment). Dissipated energy flux per active reaction centre (DI_0/RC) was increased in the -NO_3 treatment compared to the NO_3 treatment (Fig. 1 and Supplementary Fig. S1).

Performance indices (PI), both per absorbed energy (PI_{ABS}) and total (PI_{tot}) increased by the increase in NH_4^+ supply compared to nitrate supply (NO_3) (two to three times depending on the PI index type) while both indices decreased significantly in the deficient treatment (-NO_3). PI_{ABS} was much more affected by the treatments compared to the PI_{tot} index (Table 1). The difference between the two PIs is due to the stability or slight reduction of δR_0 values in NH_4 treatments (Supplementary Fig. S1), while PI_{ABS} increased. These contrasting changes resulted in a less responsive PI_{total} because it is calculated as a

function of PI_{ABS} and δR_0. That is, any improvement of photosynthetic performance is mainly due to processes described by the PI_{ABS} index.

Table 1
Photosynthetic parameters of plants of treatments NO_3, NO_3/NH_4, NH_4 and -NO_3. Chl_{tot}: total chlorophyll concentration in μg cm^{-2} (n = 6), PI_{ABS}: performance index per energy absorbed; PItot: total performance index (n = 12), A_n: net CO_2 assimilation rate in μmol CO_2 m^{-2} s^{-1}; g_s: stomatal conductance to CO_2 in mmol H_2O m^{-2} s^{-1}, E: transpiration rate in mmol H_2O m^{-2} s^{-1} (n = 6). All gas-exchange parameters presented have been measured at 550 μmol quanta m^{-2} s^{-1} (PAR) as the terminal points of the respective light-response curves. Errors are standard error of the mean. Statistically significant differences between means are marked with different letters ($P < 0.05$).

Treatment	Chl_{tot}	A_n	g_s	E	PI_{ABS}	PI_{tot}
NO_3	43.5 ± 2.5^a	4.99 ± 0.79^a	35.0 ± 4.3^a	0.62 ± 0.07^a	0.68 ± 0.08^b	0.75 ± 0.08^b
NO_3/NH_4	45.4 ± 2.9^a	4.12 ± 1.23^a	28.9 ± 7.6^a	0.53 ± 0.15^a	1.36 ± 0.22^{ab}	1.34 ± 0.09^a
NH_4	53.7 ± 4.8^a	2.92 ± 0.57^a	27.2 ± 4.1^a	0.52 ± 0.03^a	2.09 ± 0.20^a	1.35 ± 0.10^a
-NO_3	29.1 ± 1.1^b	2.38 ± 0.11^a	27.2 ± 1.3^a	0.53 ± 0.03^a	0.25 ± 0.04^c	0.58 ± 0.10^b

Anatomy, density and size of CaOx crystals

Examination of microphotographs of chlorine-bleached leaf samples revealed the expected anatomy, distribution and size of CaOx crystals in amaranth leaves (Fig. 2, NO_3 treatment; control). CaOx crystals typically occupy part of the mesophyll tissues. Normally, one to two or, less frequently, three crystals can be seen per photosynthetic compartment, as defined by leaf venation pattern. Larger crystals have a diameter around 50 μm.

The increase of NH_4^+ supply resulted in a gradual decrease of crystal size that was eventually very dramatic in the NH_4 treatment in which some crystals were very small or maybe completely absent (Fig. 2; NO_3/NH_4 and NH_4 treatments). Nitrate deficiency, on the other hand, did not cause any dramatic loss of crystals (Fig. 2; -NO_3 treatment). In these leaves, however, bleaching resulted in very notable remains of vascular bundle tissues and sheaths, probably because of low N-induced cell wall modifications (Fig. 2; -NO_3 treatment).

Quantification of chlorine-bleached leaf disk microphotographs via digital image analysis, revealed that the addition of NH_4^+ in the growth medium (NO_3/NH_4 and NH_4 treatments) not only significantly decreased size (crystal average diameter, CAD; Table 2) by 20.8 and 44.1% respectively but also decreased total volume of the crystals per leaf area (TCVA) by 53.5 and 79.2% respectively (Table 2). The changes in crystal density (CD) were not as consistent as in CAD and TCVA since it was reduced in the NO_3/NH_4 treatment by 10.3% but increased in the NH_4 treatment by 25.1%, albeit all statistically

insignificant compared to NO_3 (Table 2). Although we were cautious, there is a possibility that the reported increase in crystal density observed in the NH_4 treatment might have been erroneous, as other minor inclusions of other anatomical elements could have been mistakenly counted as crystals, due to the fact that actual CaOx crystals were also very small in size in these samples in particular (Fig. 2; NH_4 treatment).

Table 2
Calcium oxalate crystal parameters of plants of treatments NO_3, NO_3/NH_4, NH_4 and -NO_3. CD: crystal density in crystals mm^{-2}; CAD: crystal average diameter in µm; TCVA: total crystal volume per area in $\times 10^3$ μm^3 mm^{-2}; CY_{fw}: crystal yield as mg crystals g^{-1} f.w.; CY_{dw}: crystal yield as mg crystals g^{-1} d.w. Crystal yield values refer to a single combined sample (n = 1). CD, CAD and TCVA are presented as means ± standard error of the mean (n = 9). Statistically significant differences between means are marked with different letters ($P < 0.05$).

Treatment	CD	CAD	TCVA	CY_{fw}	CY_{dw}
NO_3	48.23 ± 3.71^{ab}	32.20 ± 1.42^{a}	973.1 ± 108.3^{a}	3.959	33.20
NO_3/NH_4	43.26 ± 2.21^{b}	25.49 ± 1.03^{b}	452.7 ± 45.0^{b}	2.976	22.72
NH_4	60.32 ± 4.63^{a}	18.00 ± 1.24^{c}	202.5 ± 30.4^{c}	0.611	4.61
-NO_3	47.15 ± 2.45^{b}	25.72 ± 0.66^{b}	443.0 ± 29.8^{b}	5.972	35.93

Crystal yield, leaf and root, xylem sap and nutrient solution oxalate concentration

To confirm that the observed changes in CaOx crystal size and chemical analyses (see below) are in line with the actual crystal mass, crystal yield per unit of fresh or dry biomass was determined by isolating CaOx crystals from the bulk leaf biomass of plants belonging to each one of the four treatments (pooled samples, one replicate). For the three N form treatments (NO_3, NO_3/NH_4 and NH_4), the correspondence between TCVA and crystal yield was very satisfactory (Table 2). For treatment -NO_3 the ratio between the above parameters was different owed probably to a different leaf mass per area, different chemical composition of the crystals, or less reliable data due to smaller sample size. It should be noted that the crystal yield results are purely indicative as it was not possible to analyse different replicates due to small sample size.

Leaf and root samples were analysed for soluble and insoluble oxalate by liquid chromatography. Results shown in Fig. 3 for leaf insoluble oxalate are partially in agreement with microscopic observations and crystal volume data. Leaf insoluble oxalate was reduced considerably in the NO_3/NH_4 treatment compared to the control. However, leaf insoluble oxalate in the NH_4 treatment (Fig. 3, left pane) was considerably higher than expected based on the results shown in Fig. 2 and Table 2. There are

several possible reasons for this disagreement: a) some NH_4 treatment samples might had larger CaOx crystals than the sample shown in Fig. 2. It should be noted that TCVA of the NH_4 treatment is not close to zero but still quite considerable (Table 2). b) a considerable reservoir of insoluble oxalate might have existed in the form of crystal sand located in the vascular bundle sheaths (Franceschi and Horner 1980; Karabourniotis et al. 2020), which is sometimes difficult to locate, let alone to count using digital microphotographs; in this study digital analysis of microphotographs only analysed CaOx crystals located in the mesophyll. This last possibility is strengthened by the fact that leaves of the -NO_3 treatment also showed lower TCVA than the leaves of the control plants and comparable to that of the leaves of NO_3/NH_4 treatment (Table 2), although they had the highest concentration of insoluble oxalate (Fig. 3, left pane). So, perhaps, a considerable part of insoluble oxalate in leaves of the -NO_3 treatment was also included as oxalate deposits in the very extensive vascular bundle tissues and sheath of these leaves (Fig. 2). Incidentally, roots of the -NO_3 treatment were also rich in insoluble oxalate, significantly higher from all other treatments, including control treatment, NO_3 (Fig. 3, right pane).

Leaf and root soluble oxalate concentrations were notably reduced by the increase of NH_4^+ in the nutrient solution, while -NO_3 leaves and roots had similar concentrations of soluble oxalate with the respective leaves and roots of the NO_3 treatment (Fig. 3).

Analyses of the oxalate in the nutrient solutions showed that a considerable secretion of oxalate takes place in all treatments, decreasing considerably by the increase in NH_4^+ supply compared to the NO_3 treatment (Fig. 4, left pane). Data were not corrected for any plant growth parameter such as leaf area or root biomass because plant growth was not in focus of the present study. However relative differences in oxalate secretion should not be expected to change between the three N form treatment as plant growth was similar. Nevertheless, -NO_3 plants were considerably less grown, thus oxalate secretion as presented is considerably underestimated (Fig. 4, left pane). Xylem sap oxalate showed a reducing trend, although not statistically significant, by the increase in NH_4^+ supply compared to the NO_3 treatment, while it was also not significantly different in the -NO_3 treatment compared to the control (Fig. 4, right pane).

CaOx crystal chemical composition

Micro-Raman spectral analysis of isolated crystals confirmed that are primarily composed of Ca oxalate monohydrate (COM), while a small percentage consists of Ca oxalate dihydrate (COD) or KNO_3 depending on the treatment. Specifically, only a few COD crystals were observed in all samples, with their abundance increasing as the NH_4^+ ratio increased: less than 1% in the NO_3 and NO_3/NH_4 samples and 7% in the NH_4 sample. In the sample -NO_3, COD crystals were 2%. KNO_3 crystals were detected exclusively in the NO_3 sample (22% of the total) and were absent in the NO_3/NH_4, NH_4 and -NO_3 samples (Fig. 5).

Following chemical characterization of the particles as COM, COD, or KNO_3 in the NO_3, NO_3/NH_4, NH_4, and -NO_3 samples, particle size distributions were generated for each chemical phase (Fig. 5). COM was the dominant phase in all four samples and comparable average COM diameters were observed across treatments. Specifically, the average equivalent circular diameters of COM in the NO_3, NO_3/NH_4, NH_4, and -NO_3 treatments were 36.4 µm, 35.4 µm, 33.9 µm, and 37.4 µm, respectively. For COD, the respective average diameters in the NO_3, NO_3/NH_4, NH_4, and -NO_3 treatments were 5.0 µm, 20.2 µm, 38.8 µm and 25.5 µm. While the average diameters of all particles identified as crystals in each sample using the ParticleFinder™ software (primarily those composed of COM; Fig. 5) were quite different than the average diameters measured from microphotographs (Fig. 2 and Table 2), both methods revealed a decreasing trend in crystal size with increasing NH_4^+ ratio. The reason for the relative higher values of average diameter measured by combined Micro-Raman analysis and ParticleFinder™ might be the absence of very small crystals in samples due to the isolation protocol, as crystal precipitation and subsequent washings of the pellet with isopropanol to remove cell debris likely favours the isolation of larger crystals over smaller ones.

Discussion

Effects of nitrogen nutrition on photosynthetic parameters

Nitrogen nutrition treatments differing in the ratio of NO_3^- to NH_4^+ caused several effects on parameters related to photosynthesis. A_n showed a reducing trend as the NH_4^+ ratio increased. The reason for the decrease is not clear, since chlorophylls and stomatal conductance were not much affected, while JIP-test analysis parameters were more favoured by NH_4^+ nutrition. Quantum yield of primary PSII photochemistry (φP_0), quantum yield and energy efficiency for electron transfer from Q_A to Q_B (φE_0 and ψE_0) and quantum yield of reduction of end electron acceptors at the PSI acceptor side (φR_0) were all improved with the higher increase found in φE_0 and ψE_0. Consequently, PI indices were positively affected in the NO_3/NH_4 and NH_4 treatments. Additionally, since increase of 1-V_I in NH_4 treatments indicates stronger PSI acceptor cite capacity, this could be due to higher $NADP^+$ regeneration, improved activity of Ferredoxin dependent $NADP^+$ Reductase (FNR) or Calvin cycle or activation of alternative sinks (Bota et al. 2004). Improved Calvin cycle activity is the less possible option as A_n was reduced in NH_4 treatments. Evidence of the present study also suggest the absent of stress on the photosynthetic machinery on NH_4^+ nutrition as the quantum yield of energy dissipation (φD_0) and the V_K/V_J ratio, i.e. the balance between donor-side vs. acceptor-side limitations, related to the impairment of the oxygen-evolving complex (OEC), were both reduced in NH_4^+-fed plants. ABS/RC and TR_0/RC, were reduced by NH_4^+ nutrition indicating more active PSII centres maintained under the NO_3/NH_4 and NH_4 treatments, as major modifications in antenna size are ruled out judging from the respective per cross section parameters (data not shown) (Strasser and Stirbet 2001; Strasser et al. 2004) and, despite the non-statistically significant trend for increased chlorophyll content. Moreover, the increase in ET_0/RC and the

reduction in DI_0/RC under NH_4^+ nutrition suggests a higher efficiency of conversion of trapped energy to electron transport and a lower energy dissipation (Strasser et al. 2004). In other words, decrease of NO_3/NH_4 ratio, accompanied by A_n decrease, seems to favour protection from any excess photon energy through alternative sinks of electrons, like Mehler reaction, photorespiration or nitrate reduction (φR_0, 1-V_I), rather than through heat dissipation (DI_0/RC, φD_0).

To the authors' knowledge, there is no specific information concerning the effects of NH_4^+ supply on photosynthetic parameters in *Amaranthus* species. In general, while it is commonly reported that NH_4^+ nutrition may cause toxicity, leading to increased ROS production, altered respiratory metabolism and other related perturbations, its effects on the photosynthetic process seems variable, depending on the application protocol and the level of tolerance of each genotype (Guo et al. 2007; Shilpha et al. 2023) and references therein). The reduction of A_n in combination with a comparably lower decrease or no change in stomatal parameters resulted in a notable decrease of water use efficiency (WUE; data not shown). A decreased WUE under NH_4^+ nutrition has been previously reported (Britto and Kronzucker 2013 and references therein). Inclusion of NH_4^+ in plant N supply, usually - but not always - at lower amounts compared to NO_3^-, may in turn be considered as a favourable addition for a balanced N nutrition leading to more efficient photosynthesis and, hence, plant growth ((Britto and Kronzucker 2013; Guo et al. 2007; Roosta et al. 2025; Shilpha et al. 2023; Wang et al. 2024) and references therein).

A study of photosynthesis in rice under different forms of N supply, a well-known NH_4^+ tolerant plant species (Shilpha et al. 2023), showed that photosynthetic parameters, including photochemical efficiency of PSII, between NO_3^-- and NH_4^+-fed plants were not essentially different. In addition, NH_4^+-fed plants had increased levels of chlorophylls (Ji and Peng 2005), similarly to the results of the present study. On the other hand, while balanced NO_3^-/NH_4^+ nutrition improved photochemical energy efficiency and performance indices, sole NH_4^+ nutrition reduced photochemical performance and increased oxidative stress in *Glycyrrhiza glabra* (Roosta et al. 2025). In *Schima superba*, a subtropical tree species, while photosynthetic rate and chlorophylls' concentration peaked on balanced NO_3^-/NH_4^+ nutrition, consistently with the current study, performance index (PI_{abs}) peaked on the 8:2 NH_4^+/NO_3^- ratio of N supply (Yan et al. 2025). Similar findings, to those reported here, for A_n (accompanied with a reduction in g_s, although not such high as to account for the high reduction in A_n), chlorophylls, and a higher maximum quantum yield of PSII photochemistry (F_v/F_m), which is technically the same as JIP-test's φP_0, were obtained by Roosta (2024) when pepper plants were grown on NH_4^+. Cao et al. (2023) reported similar findings in *Lonicera japonicum* for gas exchange (A_n, stomatal and mesophyll conductance and transpiration rate were all reduced), where the highest rates were recorded on NO_3^- or NO_3^-/NH_4^+ and the lowest on NH_4^+ nutrition, but chlorophyll fluorescence parameters were better when plants were grown on balanced N supply while the worst were those on NH_4^+ supply. The authors suggested the OEC and the electron flow from PSII to intersystem electron carriers as probable sites for NH_4^+ toxicity in the

photosynthetic apparatus (Cao et al. 2023). Also, *Morus alba* seedlings were grown better on balanced N supply while chlorophyll fluorescence parameters were the worst on NH_4^+ supply (Xu et al. 2022). In an extreme case of NH_4^+ sensitivity, *Solanum lycopersicon* showed progressively worse growth, chlorophyll concentration, gas exchange rates and PSII maximum quantum efficiency by increasing NH_4^+ supply with the balanced N nutrition being also worse in most parameters than sole NO_3^- nutrition (Nasraoui-Hajaji and Gouia, 2014). On the contrary, in an extreme case of NH_4^+ preference, A_n and g_s increased when *Cunninghamia lanceolata* seedlings were grown with increasing NH_4^+/NO_3^- ratios up to sole NH_4^+ compared to sole NO_3^- nutrition (Quan et al. 2024). Since no visual symptoms (including chlorophylls' concentration) or physiological disorders (other than the reduction of A_n) occurred, even at the highest NH_4^+ supply, while processes related to OEC and electron flow were positively affected, the present evidence suggests that pigweed plants were not under any degree of ammonium toxicity.

The N deficient treatment (-NO_3) exhibited severe reduction in all parameters related to photosynthesis, including chlorophylls' concentration, a reducing trend for A_n (but again not g_s and E), quantum yields and energy efficiencies and PIs. Reduction of gas exchange rate is a typical response under low N conditions (Joshi et al. 2020). In the present study, for the -NO_3 treatment, A_n reduction can easily be attributed to the lower chlorophylls, impaired PSII photochemistry, lower electron flow and lower reduction rates at the PSI acceptor side. Higher energy dissipation and partial impairment of the OEC was also evident judging from the respective parameters (φD_0, DI_0/RC, and V_K/V_J).

Effects of nitrogen nutrition on CaOx crystals and soluble oxalate

Pigweed can be classified as a facultative calcicole physiotype species based on a) the high rate of Ca absorption, b) the high capacity of precipitation of excess Ca in the form of CaOx crystals (Kinzel and Lechner 1992; Lee 1998), and c) the relatively high growth rates in different substrate pH values, in which near neutral values are more favourable than acidic ones (Singh and Whitehead 1992). However, this species shows a wide ecological amplitude that allows its establishment beyond strictly calcareous habitats, probably a good explanation for its cosmopolitan distribution (Hamidzadeh Moghadam et al. 2021). This ability, and the classification of pigweed as a facultative calcicole species, can also be established on a N-source preference, or tolerance, basis (Lee 1998), since it grows well on both NO_3^- and NH_4^+ (data not shown) and, besides the reducing trend in A_n, nearly all photochemical parameters derived from the JIP-test analysis are improved in comparison with NO_3^--grown plants, indicating that this species is tolerant to, if not favoured by, high NH_4^+ supply.

A common response of NH_4^+ nutrition is the much less oxalate accumulation compared to NO_3^--fed plants (Al Daini et al. 2013; Goyal and Kaur, 2019; Libert and Franceschi 1987; Liu et al. 2015a, b; Zhang et al. 2005) and in amaranth species in particular (Munene et al. 2017; Sriraj et al. 2022). Apart from the

well described dependence between carboxylate anions accumulation and nitrate uptake and assimilation (Raven and Smith, 1976; Xu et al. 2006), more causes can be proposed for the above response. One is the increased need for organic carbon for NH_4^+ assimilation (de la Peña et al. 2019; Hachiya and Sakakibara, 2017), which becomes less available for oxalate synthesis. The second plausible explanation is based on reports that NH_4^+ nutrition might be related to stomatal closure as a result of NH_4^+ toxicity (Torralbo et al. 2019) or nitrate deprivation which acts directly on guard cells (Kou et al. 2025). Indeed, a trend for stomatal closure was observed in the present data, albeit not statistically significant. Stomatal closure could trigger alarm photosynthesis responses that could result in reduced CaOx crystals' size as previously reported (Tooulakou et al. 2016a).

In the present study, both insoluble - despite some inconsistency between the chemically analysed and measured as CaOx crystals fraction; see Results section - and, to a greater extend, soluble oxalate, were dramatically reduced, progressively, with the increase in NH_4^+ supply. Changes in soluble oxalate in both leaf and root tissues of all treatments were, more or less, in accordance with the data for insoluble oxalate, indicating that these two pools are interchangeable. The present results are also in agreement with reports associating the N form supplied, and thus the intensity of NO_3^- reduction needed for N assimilation with oxalate accumulation for both plant parts (Liu et al. 2015b; Raven and Smith 1976; Sugiyama and Okutani 1996).

Many researchers suggest that oxalate accumulation in NO_3^--fed plants is an unwanted trait (Franceschi and Nakata 2005; Libert and Franceschi 1987). From a plant physiologist's view, however, high or exclusive ammonium-N nutrition may cause disorders in calcicole plant species (Shilpha et al. 2023). It is possible that a N-nutrition that will considerably lower oxalate content, may negatively affect some essential protective functions in which oxalate takes active part, such as nutrient acquisition and alarm photosynthesis. The extent of these interactions and their effect on stress responses and long-term acclimation ability of plants merits further examination. NH_4^+ nutrition has also been associated with increased stress tolerance, especially concerning biotic interactions, which is considered to be related to induced defence reactions owed to ROS generated by mild NH_4^+ toxicity (Shilpha et al. 2023).

Root exudation of oxalate was progressively reduced by the increase of NH_4^+ supply, judged from the concentrations of oxalate in the nutrient solutions. It has been suggested that NO_3^- assimilation metabolism leads to a build-up of carboxylates including oxalate in some species. Although CaOx crystals might be formed to isolate oxalates in favour of pH and osmotic homeostasis, oxalate root exudation might also serve to reduce oxalate overload. As seen in this study, increased concentration of oxalate in the nutrient solution, potentially resulted from root oxalate exudation. According to (Raven and Smith, 1976), in case that NO_3^- reduction is taking place in the root, root tissues might secret part of the oxalate instead of, or in parallel with, CaOx crystals' accumulation. This information is in line to the fact that root tissues in the present study did not show any difference in insoluble oxalate concentration

between the three treatments, possibly because a basic level of insoluble oxalate was not affected by the N source while soluble root tissue oxalate and oxalate exudation was affected instead.

N deficient supply in the form of NO_3^- did not result in any notable change in leaf insoluble oxalate concentrations while, in roots, a considerable increase was instead recorded. Root exudation, on the other hand, was dramatically reduced on a nutrient solution basis, probably owed to the dramatic decline of root size (data not shown). These results are in accordance with the view that while the volume of nitrate assimilation is associated with oxalate build-up, the NO_3^- supply itself is not a prerequisite for oxalate synthesis (Sugiyama and Okutani 1996).

Chemical analysis of isolated calcium oxalate crystals revealed that the ratio of COD increases by the increase in NH_4^+ supply, which is of unknown cause, to the knowledge of the authors. Although absolute amounts are not large, this should be accounted as it may have an effect on digestibility and hence bioavailability of oxalate since COD show higher solubility than COM (McBride et al. 2017).

It has been reported previously that oxalate, originating from synthesis in root tissues of pigweed, is transferred to the above ground part through the xylem (Tooulakou et al. 2016a). In the present study, xylem sap oxalate concentration showed a reducing trend by the decrease of NO_3^- supply indicating that it is possible that lower amounts of oxalate are loaded in the xylem from root cells. It is not clear, though, whether and to what extent xylem oxalate was affected by reabsorption from the nutrient solution or was defined solely by root synthesis and xylem loading. It is most probable, however, that the main source of xylem sap oxalate is from root cell metabolic processes rather than from the nutrient solution since -NO_3 plants' xylem sap oxalate content was comparable with that of other treatments despite the very low oxalate concentration in the nutrient solution.

N deficiency induces changes in cell wall synthesis by altering both the anatomy and the chemical composition of cell walls, including changes in lignification. For instance, (Hisatomi and Ueno 2025) reported that leaves of low-N *Panicum miliaceum* plants had thicker cell walls, while (Rivai et al. 2021) reported changes in cell wall composition and considerable secondary cell wall thickening for low N sorghum seedlings. This is the most probable reason for the very notable remains of vascular bundle tissues and sheaths of -NO_3 plants observed in our study in chlorine-bleached samples.

Conclusion

The N form supplied has a direct effect on synthesis and accumulation of both soluble and insoluble oxalate mainly associated with NO_3^- reduction, with these two pools appearing interchangeable. N nutrition also affects CaOx crystal size and distribution, xylem sap oxalate and oxalate root exudation. Overall physiology of pigweed is not impaired by NH_4^+ nutrition indicating its facultative calcicole physiotype and wide ecological adaptation, compatible with its cosmopolitan distribution.

Photosynthesis is affected by the N form supplied in a more complex way, revealing different behaviour in gas exchange versus photochemical processes, that merits further research.

Declarations

Acknowledgements

Authors thank Associate Professor Efi Levizou (Department of Agriculture Crop Production and Rural Environment, School of Agricultural Sciences, University of Thessaly) for Pre-Submission Review of the manuscript.

Funding Information

No funding was received for conducting this study or to assist with the preparation of this manuscript.

Author Contribution Statement

Conceptualization: G. Karabourniotis, D. Nikolopoulos, P. Bresta, G. Liakopoulos. Material preparation and experimental design: A. Matiatos , D. Nikolopoulos, P. Bresta, G. Liakopoulos. Data collection and analysis: A. Matiatos, E.-A. Kyrkoulis, O. Moutsa, M. Lykouras, M.G. Orkoula, C.G. Kontoyannis. Statistical analysis: P. Bresta. First draft: G. Karabourniotis, G. Liakopoulos. Review and editing: D. Nikolopoulos, P. Bresta, G. Grammatikopoulos, M.G. Orkoula. All authors read and approved the final manuscript.

Conflict of interests

The authors declare that they have no conflict of interest.

Data availability

The datasets generated during and/or analysed during the current study are available from the corresponding author on reasonable request.

References

1. Al Daini H, Norman HC, Young P, Barrett-Lennard EG (2013) The source of nitrogen (NH_4^+ or NO_3^-) affects the concentration of oxalate in the shoots and the growth of *Atriplex nummularia* (oldman saltbush). Funct Plant Biol **40**: 1057–1064. https://doi.org/10.1071/FP13060
2. Bota J, Medrano H, Flexas J 2004 Is photosynthesis limited by decreased Rubisco activity and RuBP content under progressive water stress? New Phytol **162**: 671–681. https://doi.org/10.1111/j.1469-8137.2004.01056.x
3. Bothe H 2015. The lime-silicate question. Soil Biol Biochem **89**: 172–183. https://doi.org/10.1016/j.soilbio.2015.07.004

4. Britto DT, Kronzucker HJ 2013 Ecological significance and complexity of N-source preference in plants. Ann Bot **112**: 957–963. https://doi.org/10.1093/aob/mct157
5. Cao Y, Pan Y, Wang M, Liu T, Meng X, Guo S 2023 The effects of different nitrogen forms on chlorophyll fluorescence and photosystem II in *Lonicera japonica*. J Plant Growth Regul **42**: 4106–4117. https://doi.org/10.1007/s00344-022-10873-1
6. Ceppi MG, Oukarroum A, Çiçek N, Strasser RJ, Schansker G 2011 The IP amplitude of the fluorescence rise OJIP is sensitive to changes in the photosystem I content of leaves: A study on plants exposed to magnesium and sulfate deficiencies, drought stress and salt stress. Physiol Plant **144**: 277–288. https://doi.org/10.1111/j.1399-3054.2011.01549.x
7. de la Peña M, González-Moro MB, Marino D 2019 Providing carbon skeletons to sustain amide synthesis in roots underlines the suitability of *Brachypodium distachyon* for the study of ammonium stress in cereals. AoB Plants **11**: plz029. https://doi.org/10.1093/aobpla/plz029
8. Franceschi VR 1987 Oxalic acid metabolism and calcium oxalate formation in *Lemna minor* L. Plant Cell Environ **10**: 397–406. https://doi.org/10.1111/1365-3040.ep11603639
9. Franceschi VR, Horner HT Jr 1980 Calcium oxalate crystals in plants. Bot Rev **46**: 361–427. https://doi.org/10.1007/BF02860532
10. Franceschi VR, Nakata PA 2005 Calcium oxalate in plants: Formation and function. Ann Rev Plant Biol **56**: 41–71. https://doi.org/10.1146/annurev.arplant.56.032604.144106
11. Goyal M, Kaur R 2019 Interactive effect of nitrogen nutrition, nitrate reduction and seasonal variation on oxalate synthesis in leaves of Napier-bajra hybrid (*Pennisetum purpureum* × *P. glaucum*). Crop Pasture Sci **70**: 669–675. https://doi.org/10.1071/CP18282
12. Guo S, Zhou Y, Shen Q, Zhang F 2007 Effect of ammonium and nitrate nutrition on some physiological processes in higher plants - growth, photosynthesis, photorespiration, and water relations. Plant Biol **9**: 21–29. https://doi.org/10.1055/s-2006-924541
13. Hachiya T, Sakakibara H 2017 Interactions between nitrate and ammonium in their uptake, allocation, assimilation, and signaling in plants. J Exp Bot **68**: 2501–2512. https://doi.org/10.1093/jxb/erw449
14. Hammer Ø, Harper DAT, Ryan PD 2001 PAST: paleontological statisticssoftware package for education and data analysis. Palaeont Electr **4**: 1–9. https://palaeo-electronica.org/2001_1/past/issue1_01.htm
15. Hamidzadeh Moghadam S, Alebrahim MT, Tobeh A, Mohebodini M, Werck-Reichhart D, MacGregor DR, Tseng TM 2021 Redroot pigweed (*Amaranthus retroflexus* L.) and lamb's quarters (*Chenopodium album* L.) populations exhibit a high degree of morphological and biochemical diversity. Front Plant Sci **12**: 593037. https://doi.org/10.3389/fpls.2021.593037
16. Hisatomi H, Ueno O 2025 Influence of nitrogen deficiency on leaf anatomy, organelle quantities, and photosynthetic traits of the NAD-ME type C_4 grass, *Panicum miliaceum* (common millet). Plant Prod Sci **28**: 242–256. https://doi.org/10.1080/1343943X.2025.2510928

17. Ji X-M, Peng X-X 2005 Oxalate accumulation as regulated by nitrogen forms and its relationship to photosynthesis in rice (*Oryza sativa* L.). *Journal of Integrative* Plant Biol **47**: 831–838. https://doi.org/10.1111/j.1744-7909.2005.00099.x
18. Jones DL 1998 Organic acids in the rhizosphere - A critical review. Plant Soil **205**: 25–44. https://doi.org/10.1023/A:1004356007312
19. Joshi V, Joshi M, Penalosa A 2020 Comparative analysis of tissue-specific transcriptomic responses to nitrogen stress in spinach (*Spinacia oleracea*). PLoS ONE **15**: e0232011. https://doi.org/10.1371/journal.pone.0232011
20. Karabourniotis G, Horner HT, Bresta P, Nikolopoulos D, Liakopoulos G 2020 New insights into the functions of carbon–calcium inclusions in plants. New Phytol **228**: 845–854. https://doi.org/10.1111/nph.16763
21. Kinzel H, Lechner I 1992 The specific mineral metabolism of selected plant species and its ecological implications. Bot Acta **105**: 355–361. https://doi.org/10.1111/j.1438-8677.1992.tb00312.x
22. Kou Y, Su B, Yang S, Gong W, Zhang X, Shan X 2025 Phosphorylation of *Arabidopsis* NRT1.1 regulates plant stomatal aperture and drought resistance in low nitrate condition. BMC Plant Biol **25**: 95. https://doi.org/10.1186/s12870-024-06008-1
23. Kumar V, Irfan M, Datta A 2019 Manipulation of oxalate metabolism in plants for improving food quality and productivity. Phytochemistry **158**: 103–109. https://doi.org/10.1016/j.phytochem.2018.10.029
24. Lambers H, Chapin III FS, Pons TL 2019 Plant Physiological Ecology. Springer Cham. https://doi.org/10.1007/978-3-030-29639-1
25. Lee JA 1998 The calcicole-calcifuge problem revisited. Adv Bot Res **29(c)**: 1–30. https://doi.org/10.1016/S0065-2296(08)60306-7
26. Li P, Liu C, Luo Y, Shi H, Li Q, Pinchu C, Li X, Yang J, Fan W 2022 Oxalate in plants: metabolism, function, regulation, and application. J Agric Food Chem **70**: 16037–16049. https://doi.org/10.1021/acs.jafc.2c04787
27. Libert B, Franceschi VR 1987 Oxalate in crop plants. J Agric Food Chem **35**: 926–938. https://doi.org/10.1021/jf00078a019
28. Lichtenthaler HK 1987 Chlorophylls and Carotenoids: Pigments of Photosynthetic Membranes. In: Colowick SP and Kaplan NO (eds) Methods in Enzymology, Vol. 148, Academic Press, San Diego, 350–382. https://doi.org/10.1016/0076-6879(87)48036-1
29. Liu X, Lu L, Chen Q, Ding W, Dai P, Hu Y, Yu Y, Jin C, Lin X 2015a Ammonium reduces oxalate accumulation in different spinach (*Spinacia oleracea* L.) genotypes by inhibiting root uptake of nitrate. Food Chem **186**: 312–318. https://doi.org/10.1016/j.foodchem.2014.06.122
30. Liu XX, Zhou K, Hu Y, Jin R, Lu LL, Jin CW, Lin XY 2015b Oxalate synthesis in leaves is associated with root uptake of nitrate and its assimilation in spinach (*Spinacia oleracea* L.) plants. J Sci Food Agric **95**: 2105–2116. https://doi.org/10.1002/jsfa.6926

31. Marschner H 1974 Calcium nutrition of higher plants. Neth J Agric Sci **22**: 275–282. https://doi.org/10.18174/njas.v22i4.17212
32. Massey LK 2003 Dietary influences on urinary oxalate and risk of kidney stones. Front Biosci **8 (SUPPL.)**: 584–594. https://doi.org/10.2741/1082
33. McBride MB, Frenchmeyer M, Kelch SE, Aristilde L 2017 Solubility, structure, and morphology in the co-precipitation of cadmium and zinc with calcium-oxalate. J Colloid Interface Sci **486**: 309–315. https://doi.org/10.1016/j.jcis.2016.09.079
34. Michalet R, Gandoy C, Joud D, Pagès J-P, Choler P 2002 Plant community composition and biomass on calcareous and siliceous substrates in the northern French Alps: Comparative effects of soil chemistry and water status. Arct Antarct Alp Res **34**: 102–113. https://doi.org/10.1080/15230430.2002.12003474
35. Morita A, Suzuki R, Yokota H 2004 Effect of ammonium application on the oxalate content of tea plants (*Camellia sinensis* L.). Soil Sci Plant Nutr **50**: 763–769. https://doi.org/10.1080/00380768.2004.10408533
36. Munene R, Changamu E, Korir N, Gweyi-Onyango JP 2017 Differential impact of nitrogen forms on selected phytochemicals and oxalate contents in three vegetable amaranth varieties in Kenya. Ann Food Sci Technol **18**: 238–246. http://ir-library.ku.ac.ke/handle/123456789/18112
37. Nakata PA 2012 Influence of calcium oxalate crystal accumulation on the calcium content of seeds from *Medicago truncatula*. Plant Sci **185–186**: 246–249. https://doi.org/10.1016/j.plantsci.2011.11.009
38. Nasraoui-Hajaji A, Gouia H 2014 Photosynthesis sensitivity to NH_4^+-N change with nitrogen fertilizer type. Plant Soil Environ **60**: 274–279. https://doi.org/10.17221/7418-PSE
39. Nemer D, Liancourt P, Delerue F, Randé H, Michalet R 2021 Species stress tolerance and community competitive effects drive differences in species composition between calcareous and siliceous plant communities. J Ecol **109**: 4132–4142. https://doi.org/10.1111/1365-2745.13785
40. Paiva EAS 2019 Are calcium oxalate crystals a dynamic calcium store in plants? New Phytol **223**: 1707–1711. https://doi.org/10.1111/nph.15908
41. Palmieri F, Estoppey A, House GL, Lohberger A, Bindschedler S, Chain PSG, Junier P 2019 Oxalic acid, a molecule at the crossroads of bacterial-fungal interactions. Adv Appl Microbiol **106**: 49–77. https://doi.org/10.1016/bs.aambs.2018.10.001
42. Peña N, Minguez S, Escobar JD 2024 Current production scenario and functional potential of the whole amaranth plant: A review. In: Pseudocereals-Recent Advances and New Perspectives. Waisundara VY (ed.). IntechOpen. https://doi.org/10.5772/intechopen.107794
43. Prychid CJ, Rudall PJ 1999 Calcium oxalate crystals in monocotyledons: a review of their structure and systematics. Ann Bot **84**: 725–739. https://doi.org/10.1006/anbo.1999.0975
44. Quan X-Q, Wang Y-R, Li X-Y, Liang H-Y, Wang L-D, Yan X-L 2024 Effects of nitrogen addition level and NH_4^+-N to NO_3^--N ratio on photosynthetic characteristics and chlorophyll fluorescence parameters

in *Cunninghamia lanceolata* seedling. Chin J Plant Ecol **48**: 1050–1064. https://doi.org/10.17521/cjpe.2023.0200

45. Raven JA, Smith FA 1976 Nitrogen assimilation and transport in vascular land plants in relation to intracellular pH regulation. New Phytol **76**: 415–431. https://doi.org/10.1111/j.1469-8137.1976.tb01477.x
46. Rivai RR, Miyamoto T, Awano T, Takada R, Tobimatsu Y, Umezawa T, Kobayashi M 2021 Nitrogen deficiency results in changes to cell wall composition of sorghum seedlings. Sci Rep **11**: 23309. https://doi.org/10.1038/s41598-021-02570-y
47. Roosta HR 2024 The responses of pepper plants to nitrogen form and dissolved oxygen concentration of nutrient solution in hydroponics. BMC Plant Biol **24**: 281. https://doi.org/10.1186/s12870-024-04943-7
48. Roosta HR, Estaji A, Khadivi A, Shams M 2025 Balanced ammonium-nitrate nutrition enhances photosynthetic efficiency, micronutrient homeostasis, and antioxidant networks via ROS signaling in *Glycyrrhiza glabra* across soil and soilless systems. Sci Rep, **15**: 25404. https://doi.org/10.1038/s41598-025-11181-w
49. Savage GP, Dubois M 2006 The effect of soaking and cooking on the oxalate content of taro leaves. Inter J Food Sci Nutr **57**: 376–381. https://doi.org/10.1080/09637480600855239
50. Shilpha J, Song J, Jeong BR 2023 Ammonium phytotoxicity and tolerance: an insight into ammonium nutrition to improve crop productivity. Agronomy **13**: 1487. https://doi.org/10.3390/agronomy13061487
51. Singh BP, Whitehead WF 1992 Response of vegetable amaranth to differing soil pH and moisture regimes. Acta Hortic **318**: 225–230. https://doi.org/10.17660/ActaHortic.1992.318.30
52. Sriraj P, Toomsan B, Butnan S 2022 Effects of neem seed extract on nitrate and oxalate contents in amaranth fertilized with mineral fertilizer and cricket frass. Horticulturae **8**: 898. https://doi.org/10.1071/CP18282
53. Stirbet A, Lazár D, Kromdijk J, Govindjee 2018 Chlorophyll a fluorescence induction: Can just a one-second measurement be used to quantify abiotic stress responses? Photosynthetica **56**: 86–104. https://doi.org/10.1007/s11099-018-0770-3
54. Stirbet A, Govindjee 2011 On the relation between the Kautsky effect (chlorophyll a fluorescence induction) and Photosystem II: Basics and applications of the OJIP fluorescence transient. *J Photochem Photobiol B Biol*, **104**: 236–257. https://doi.org/10.1016/j.jphotobiol.2010.12.010
55. Strasser RJ, Stirbet AD 2001 Estimation of the energetic connectivity of PSII centres in plants using the fluorescence rise O-J-I-P: Fitting of experimental data to three different PSII models. Math Comput Simul **56**: 451–461. https://doi.org/10.1016/S0378-4754(01)00314-7
56. Strasser RJ, Tsimilli-Michael M, Srivastava A 2004 Analysis of the Chlorophyll a Fluorescence Transient. In: Chlorophyll a Fluorescence: A Signature of Photosynthesis. Papageorgiou C and Govindjee (eds). Springer. https://doi.org/10.1007/978-1-4020-3218-9_12

57. Ström L 1997 Root exudation of organic acids: Importance to nutrient availability and the calcifuge and calcicole behaviour of plants. Oikos **80**: 459–466. https://doi.org/10.2307/3546642
58. Sugiyama N, Okutani I 1996 Relationship between nitrate reduction and oxalate synthesis in spinach leaves. J Plant Physiol **149**: 14–18. https://doi.org/10.1016/S0176-1617(96)80214-0
59. Tian H, Jiang L, Liu E, Zhang J, Liu F, Peng X 2008 Dependence of nitrate-induced oxalate accumulation on nitrate reduction in rice leaves. Physiol Plant **133**: 180–189. https://doi.org/10.1111/j.1399-3054.2008.01052.x
60. Tooulakou G, Giannopoulos A, Nikolopoulos D, Bresta P, Dotsika E, Orkoula MG, Kontoyannis CG, Fasseas C, Liakopoulos G, Klapa MI, Karabourniotis G 2016a Alarm photosynthesis: Calcium oxalate crystals as an internal CO_2 source in plants. Plant Physiol **171**: 2577–2585. https://doi.org/10.1104/pp.16.00111
61. Tooulakou G, Giannopoulos A, Nikolopoulos D, Bresta P, Dotsika E, Orkoula MG, Kontoyannis CG, Fasseas C, Liakopoulos G, Klapa MI, Karabourniotis G 2016b Reevaluation of the plant “gemstones”: Calcium oxalate crystals sustain photosynthesis under drought conditions. Plant Sign Behav **11**: e1215793. https://doi.org/10.1080/15592324.2016.1215793
62. Tooulakou G, Nikolopoulos D, Dotsika E, Orkoula MG, Kontoyannis CG, Liakopoulos G, Klapa MI, Karabourniotis G 2019 Changes in size and composition of pigweed (*Amaranthus hybridus* L.) calcium oxalate crystals under CO_2 starvation conditions. Physiol Plant **166**: 862–872. https://doi.org/10.1111/ppl.12843
63. Torralbo F, González-Moro MB, Baroja-Fernández E, Aranjuelo I, González-Murua C 2019 Differential regulation of stomatal conductance as a strategy to cope with ammonium fertilizer under ambient versus elevated CO_2. Front Plant Sci **10**: 597. https://doi.org/10.3389/fpls.2019.00597
64. Tyler G, Ström L 1995 Differing organic acid exudation pattern explains calcifuge and acidifuge behaviour of plants. Ann Bot **75**: 75–78. https://doi.org/10.1016/S0305-7364(05)80011-3
65. Wang T-C, Wei T-Y, Yeh D-M 2024 Nitrogen requirement and nitrogen form preference by *Radermachera hainanensis* and *R. sinica* plug seedlings. J Environ Hortic **42**: 117–123. https://doi.org/10.24266/0738-2898-42.3.117
66. White PJ, Broadley MR 2003 Calcium in plants. Ann Bot **92**: 487–511. https://doi.org/10.1093/aob/mcg164
67. Xu H-W, Ji X-M, He Z-H, Shi W-P, Zhu G-H, Niu J-K, Li B-S, Peng X-X 2006 Oxalate accumulation and regulation is independent of glycolate oxidase in rice leaves. J Exp Bot **57**: 1899–1908. https://doi.org/10.1093/jxb/erj131
68. Xu N, Yu SP, Ding JN, Shi CQ 2022 Response of the PS II function of *Morus alba* var. 'Qiuyu' seedling leaves to different nitrogen forms. Appl Ecol Environ Res **20**: 2157–2170. https://doi.org/10.15666/aeer/2003_21572170
69. Yan X-L, Liu G-M, Li X-Y, Jiang Y-X, Quan X-Q, Wang Y-R, Qu L-P, Tang X-H 2025 Photosynthetic characteristics and chlorophyll fluorescence parameters in *Schima superba* seedlings under

different level of nitrogen addition and NH_4^+-N to NO_3^--N ratio. Chin J Plant Ecol **49**: 624–637. https://doi.org/10.17521/cjpe.2024.0379

70. Zhang Y, Lin X, Zhang Y, Shao JZ, Du S 2005 Effects of nitrogen levels and nitrate/ammonium ratios on oxalate concentrations of different forms in edible parts of spinach. J Plant Nutr **28**: 2011–2025. https://doi.org/10.1080/01904160500311086

Figures

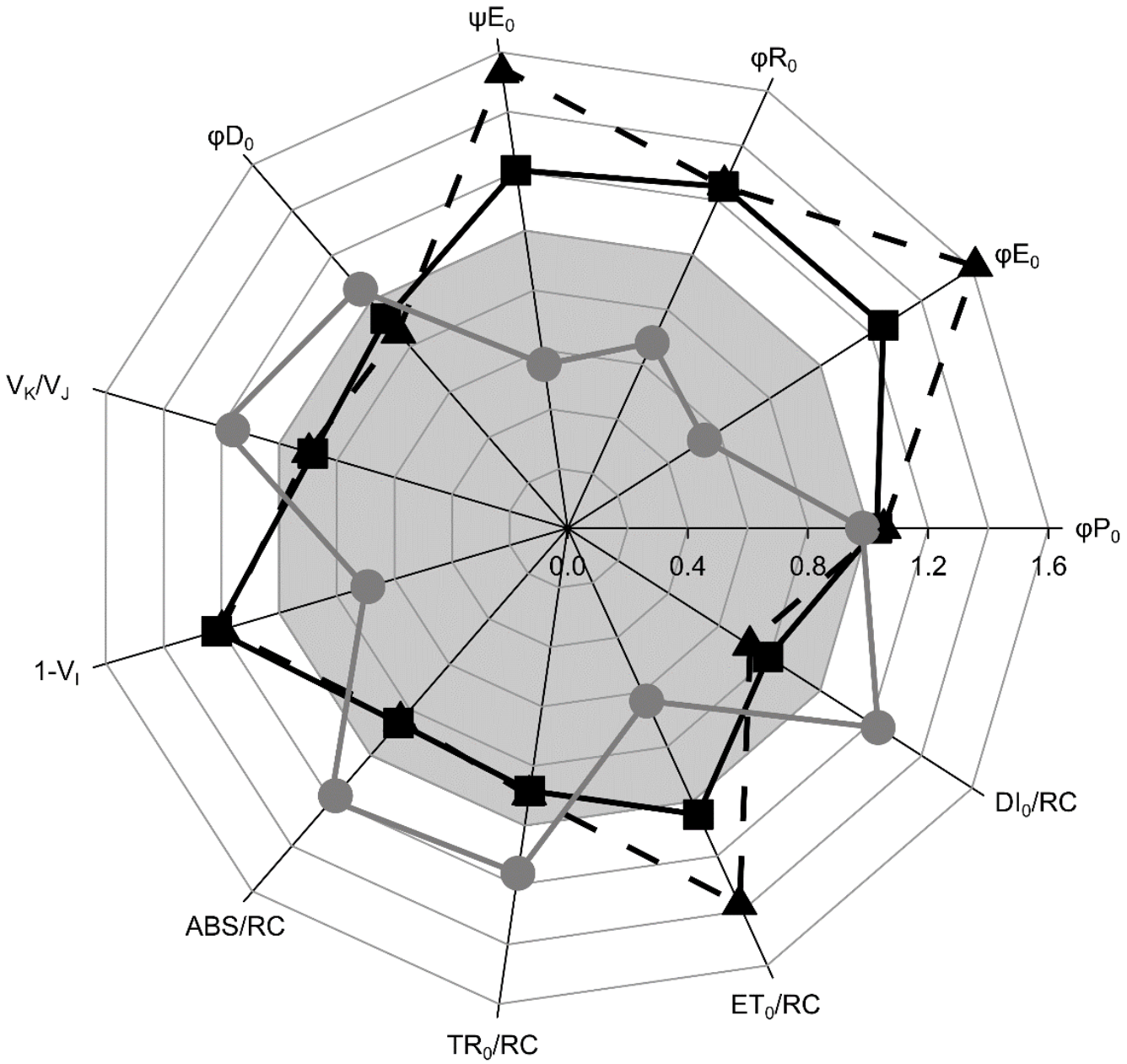

Figure 1

Parameters of light reactions according to the JIP-test analysis. For symbols see Materials and Methods. Values are normalized means (n=12) with value of treatment NO_3 set at 1 for each parameter (light grey area). Other treatments: NO_3/NH_4 solid black line/squares; NH_4 dashed black line/triangles; -NO_3 solid grey line/circles. For actual parameter values, standard errors and statistics see supplementary figure S1.

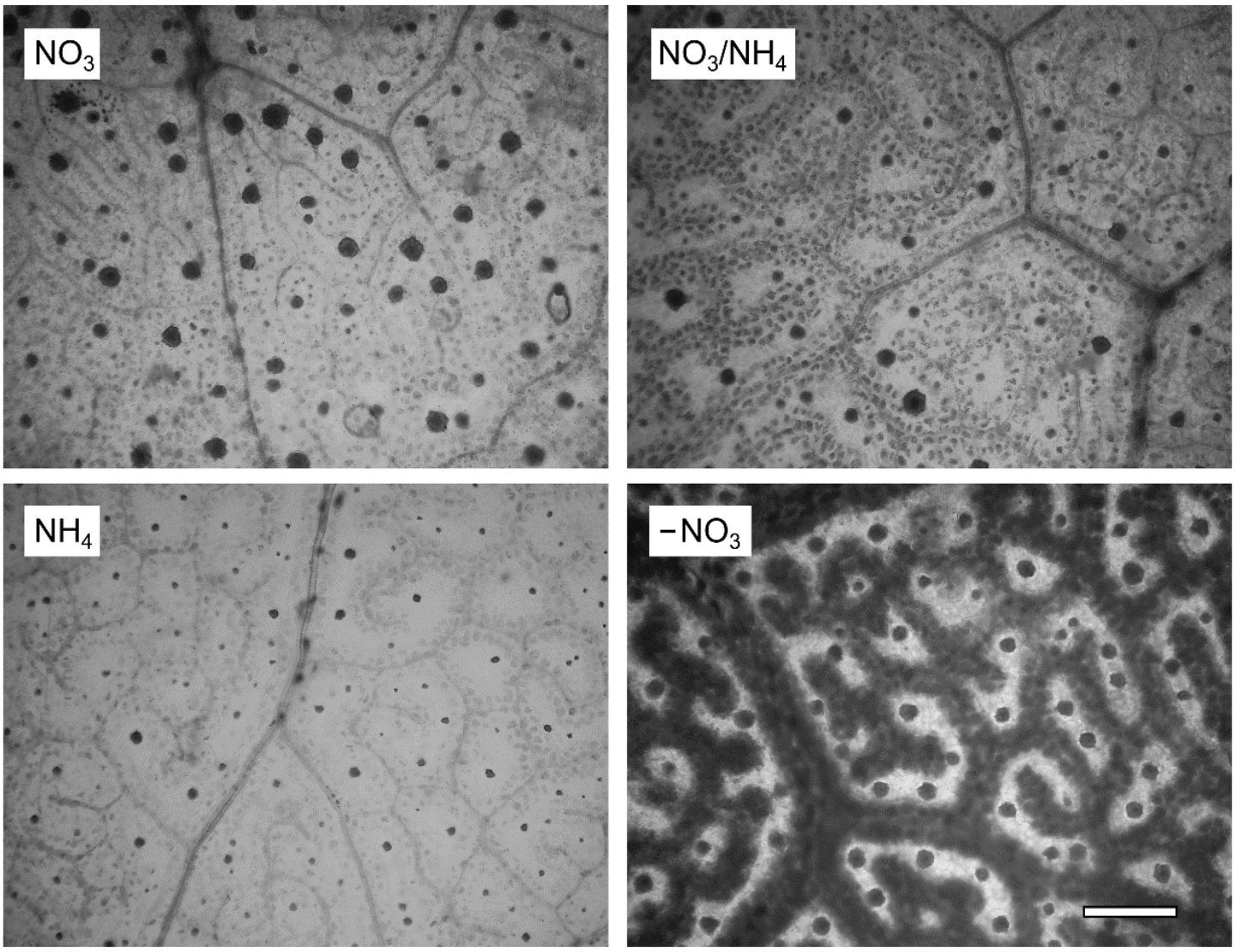

Figure 2

Microphotographs of chlorine-bleached leaf disks depicting crystal distribution and size. Leaf samples were chosen as typical of the four treatments. Bar = 200 µm.

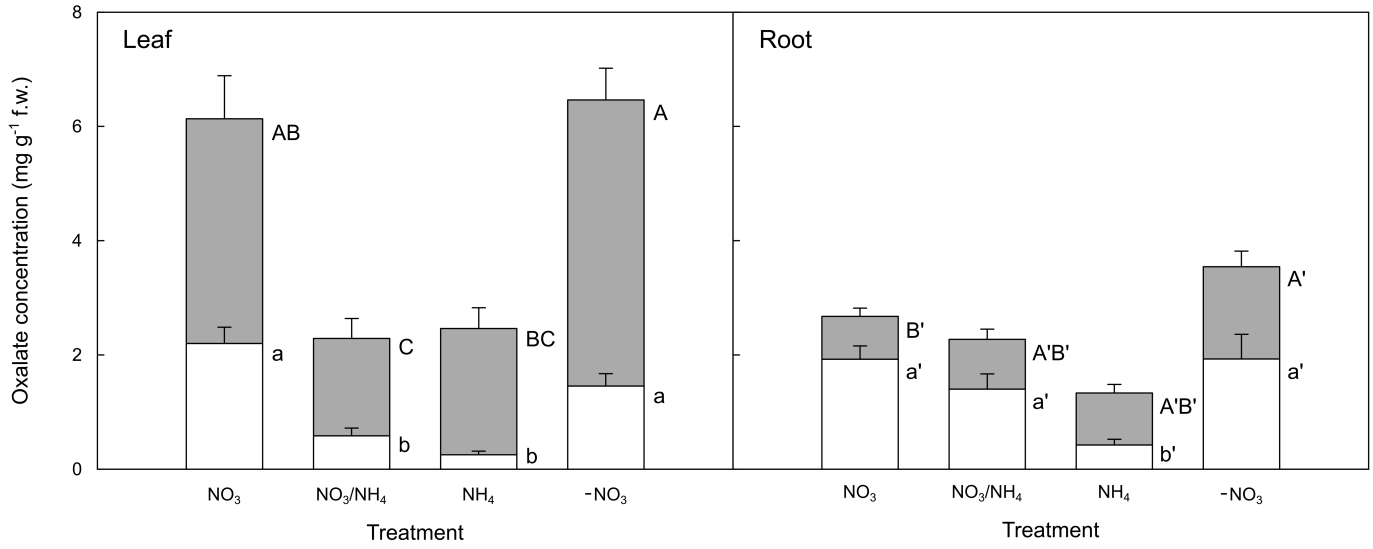

Figure 3

Leaf and root tissue insoluble (grey bars) and soluble (white bars) oxalate concentration. Error bars are standard error of the mean (n=6). Statistically significant differences between means are marked with different letters (P<0.05). Comparisons between forms of oxalate and plant organs are independent as indicated by different lettersets.

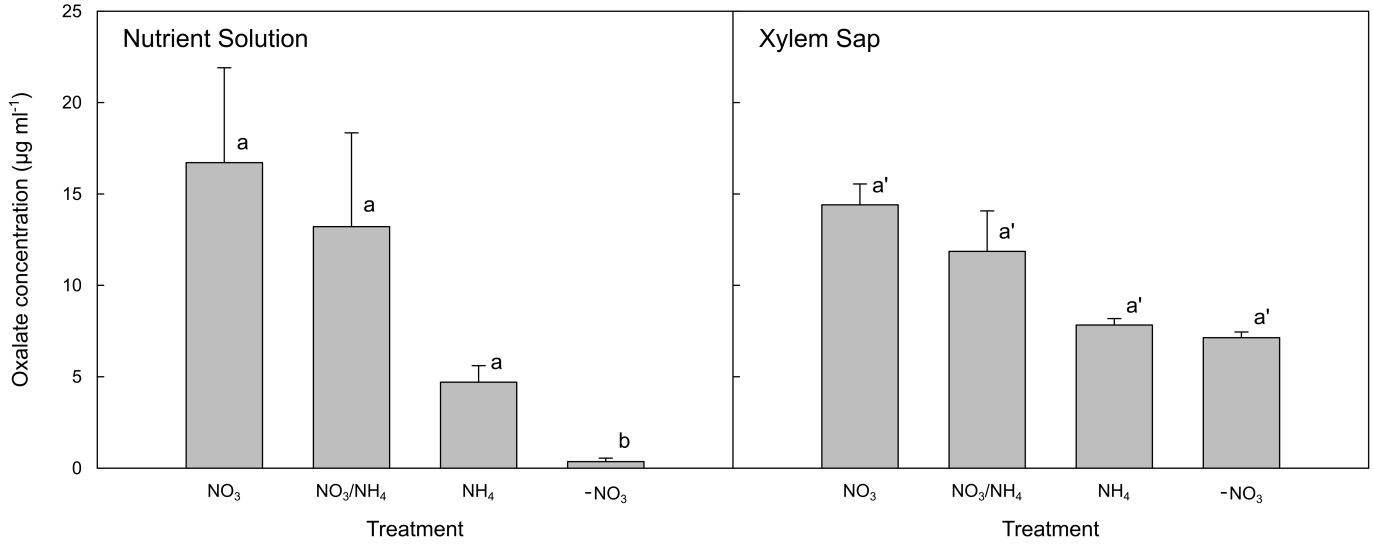

Figure 4

Nutrient solution and xylem sap oxalate concentration. Error bars are standard error of the mean (n=6 for nutrient solution analysis; n=6, 5, 4 or 2 for xylem sap analysis of treatments NO_3, NO_3/NH_4, NH_4 and -NO_3 respectively). Statistically significant differences between means are marked with different letters

(P<0.05). Comparisons for nutrient solutions and xylem sap samples are independent as indicated by different lettersets.

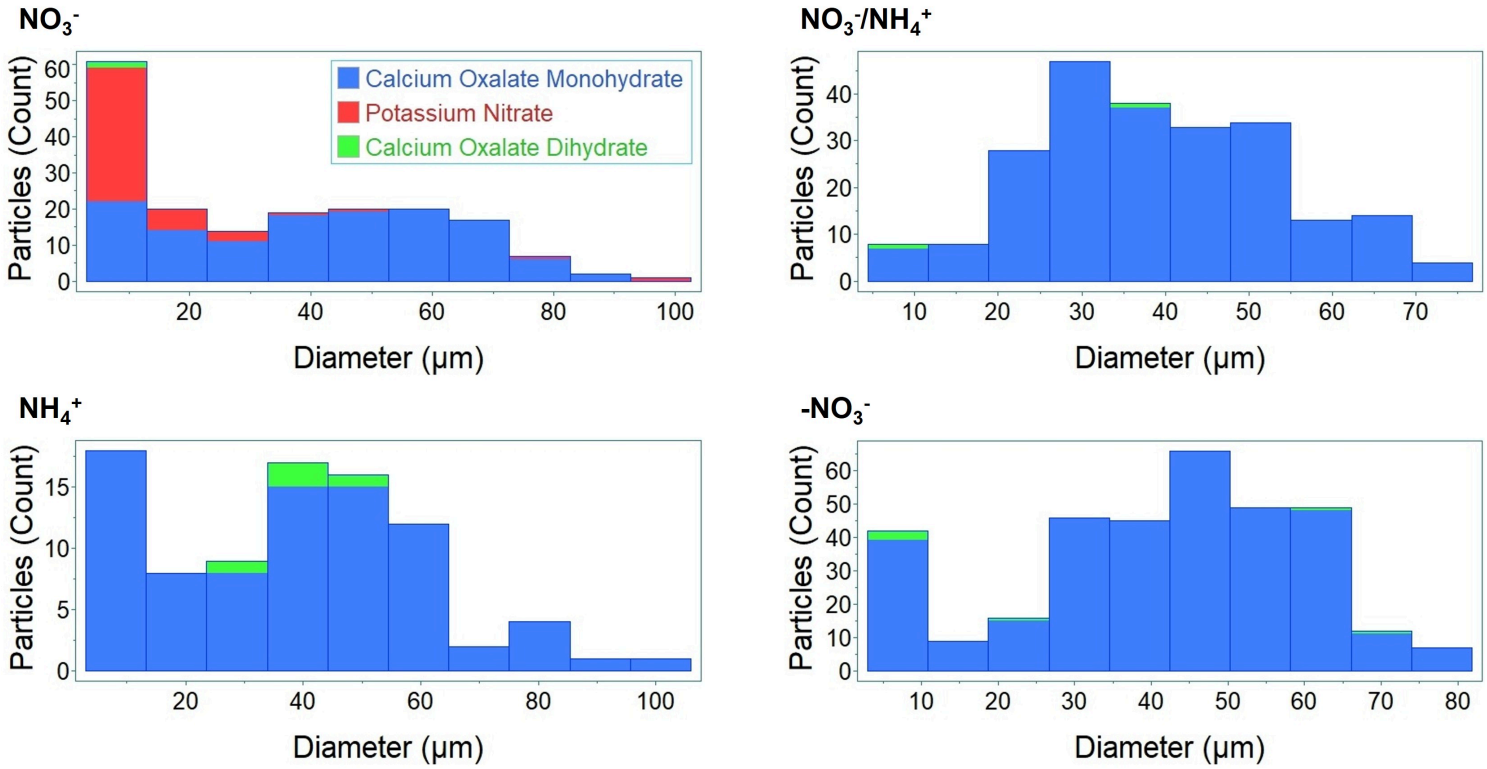

Figure 5

Chemical identification and particle size distributions of calcium oxalate monohydrate (COM; blue), calcium oxalate dihydrate (COD; green), and KNO_3 (red) in the NO_3 (upper left), NO_3/NH_4 (upper right), NH_4 (lower left), and $-NO_3$ (lower right) treatments, as determined by micro-Raman spectroscopy coupled with ParticleFinder™ analysis.

Supplementary Files

This is a list of supplementary files associated with this preprint. Click to download.

- FigureS1.pdf